Analyses of electron runaway in front of the negative streamer channel

Babich, L. P.; Bochkov, E. I.; Kutsyk, I. M.; Neubert, Torsten; Chanrion, Olivier

Published in:
Journal of Geophysical Research: Space Physics

Link to article, DOI:
10.1002/2017JA023917

Publication date:
2017

Document Version
Publisher's PDF, also known as Version of record

AGU PUBLICATIONS

JGR

Journal of Geophysical Research: Space Physics

RESEARCH ARTICLE
10.1002/2017JA023917

Key Points:
- Focusing of the ionization wave, propagating along a trail of a previous streamer allows the electric field intensity to reach magnitudes required for a generation of significant numbers of runaway electrons (REs)
- The ionization produced by the REs creates an ionized channel that allows for the ionization wave propagation self-sustained with the RE generation independent of the initial electron concentration ahead of the wave front
- Streamer coronas of the leaders are sources of REs producing the observed X-ray and γ-ray emissions

Correspondence to:
L. P. Babich,
leonid.babich52@gmail.com

Citation:
Babich, L. P., E. I. Bochkov, I. M. Kutsyk, T. Neubert, and O. Chanrion (2017), Analyses of electron runaway in front of the negative streamer channel, *J. Geophys. Res. Space Physics*, *122*, 8974–8984, doi:10.1002/2017JA023917.

Received 28 JAN 2017
Accepted 3 AUG 2017
Accepted article online 11 AUG 2017
Published online 29 AUG 2017

Analyses of electron runaway in front of the negative streamer channel

L. P. Babich[1], E. I. Bochkov[1], I. M. Kutsyk[1], T. Neubert[2], and O. Chanrion[2]

[1]Russian Federal Nuclear Center, Sarov, Russia, [2]National Space Institute, Technical University of Denmark, Lyngby, Denmark

Abstract X-ray and γ-ray emissions, observed in correlation with negative leaders of lightning and long sparks of high-voltage laboratory experiments, are conventionally connected with the bremsstrahlung of high-energy runaway electrons (REs). Here we extend a focusing mechanism, analyzed in our previous paper, which allows the electric field to reach magnitudes, required for a generation of significant RE fluxes and associated bremsstrahlung, when the ionization wave propagates in a narrow, ionized channel created by a previous streamer. Under such conditions we compute the production rate of REs per unit streamer length as a function of the streamer velocity and predict that, once a streamer is formed with the electric field capable of producing REs ahead of the streamer front, the ionization induced by the REs is capable of creating an ionized channel that allows for self-sustained propagation of the RE-emitting ionization wave independent of the initial electron concentration. Thus, the streamer coronas of the leaders are probable sources of REs producing the observed high-energy radiation. To prove these predictions, new simulations are planned, which would show explicitly that the preionization in front of the channel via REs will lead to the ionization wave propagation self-consistent with RE generation.

Plain Language Summary X-ray and γ-ray emissions, observed in correlation with the negative leaders of lightning and long sparks of high-voltage laboratory experiments, are conventionally connected with the bremsstrahlung of high-energy runaway electrons (REs). Here we extend a focusing mechanism, analyzed in our previous paper, which allows the electric field to reach magnitudes, required for a generation of significant RE fluxes and associated bremsstrahlung, when the ionization wave propagates in a narrow, ionized channel created by a previous streamer. Under such conditions we compute the production rate of REs per unit streamer length as a function of the streamer velocity and find that, once a streamer is formed with the electric field capable of producing REs ahead of the streamer front, the ionization induced by the REs creates an ionized channel that allows for self-sustained propagation of the RE-emitting ionization wave independent of the initial electron concentration. Thus, the streamer coronas of the leaders are probable sources of REs producing the observed high-energy radiation.

1. Introduction

This work extends the formulation in *Babich et al*. [2014a, 2015], describing a mechanism whereby the electric field in the streamer corona of negative leaders of lightning and long laboratory spark is enhanced to a level allowing a production of the X- and γ-ray emissions, as observed in a correlation with natural lightning and in high-voltage laboratory experiments [*Dwyer et al*., 2004, 2005, 2008, 2012a, 2012b; *Nguyen et al*., 2008; *Rahman et al*., 2008; *March and Montanya*, 2010; *Kochkin et al*., 2012, 2014, 2015; *Ostgaard et al*., 2016; *Agafonov et al*., 2013]. The radiation is the bremsstrahlung of high-energy runaway electrons (REs), for which production strong electric fields are required. Direct sensor measurements of electric field inside the leaders or streamers are not possible even in the controlled laboratory discharges due to too small spatial and temporal scales of the domains occupied by the field; therefore, the X- and γ-ray emissions are the only evidence that the electric field intensity reduced to the number density of neutrals E/N during the leader/streamer processes is increased significantly above the reduced intensity of the external field $(E/N)_{ext}$, which is too low for electrons to be energized to the levels allowing the high-energy emissions.

It is known that leaders consist of a hot plasma channel with the streamer corona at the leader tip. Lightning negative leaders and upward positive leaders have been shown experimentally to propagate in a stepwise manner [*Rakov and Uman*, 2003, sections 5.3.2 and 5.3.3; *Dwyer et al*., 2005; *Bazelyan and Raizer*, 2000, section 3.1, and citations therein]. Downward positive leaders have been observed to pulse, which suggests that they may also step [*Wang and Takagi*, 2011; *Rakov and Uman*, 2003, sections 5.3.2 and 5.3.3], but this has yet to be

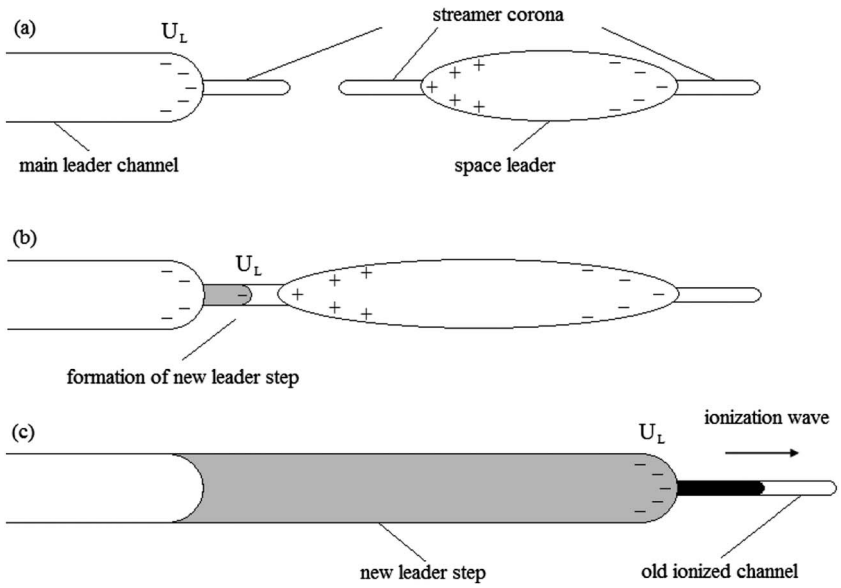

Figure 1. Illustration from *Babich et al*. [2014a, 2015] of the scenario of the negative leader development by *Bazelyan and Raizer* [2000, section 2.7]. (a) The main negative leader channel and the space leader channel with their streamer coronas. (b) Contact of the streamer coronas of the main leader (negative) and the space leader (positive) with the potential of the main leader head U_L being transferred to the space leader. (c) The potential of the old main leader is transferred to the negative tip of the space leader, launching an ionization wave propagating into the preexisting streamer channel.

explicitly demonstrated or observed. Principles of the stepping process were formulated by *Gorin et al*. [1976]; its mechanism was studied by observations of rocket-and-wire triggered lightning discharge [*Biagi et al*., 2010, 2011, 2014].

Because the field is very weak within the highly conductive hot leader channel, the analyses carried out in this paper are limited to further development of the so-called "thermal" [*Moss et al*., 2006] or "cold" [*Dwyer*, 2004] runaway in strong electric fields that may occur at heads of streamers constituting the leader corona. The field in the corona of the previous (old) step must be increased to a level that allows the RE generation before the field in this region is reduced by the next step and is reformed at the new tip location.

However, streamers, in initially unionized media, experience strong transversal expansion, which limits the field intensity to very low level [*Raizer and Simakov*, 1998]. Therefore, *Babich et al*. [2014a, 2015] proposed that if the leader corona consists of narrow ionized channels, such as formed by streamers, new ionization waves propagating in such channels allow overcoming this limitation. They noted that the limitation of the electric field magnitude due to the transversal streamer expansion can be removed because the secondary ionization waves, propagating in already ionized media, tend to focus. Focusing is a result of ionization wave velocity decrease with the ionization degree decrease [*Bazelyan and Raizer*, 1998, section 3.1.3]. As the electron concentration in a streamer channel decreases from the inner domain to its periphery, the secondary ionization wave propagates with the highest velocity at the center of the channel. Therefore, the transverse expansion of the ionization wave occurs much slower than the longitudinal wave propagation, and the wave transverse size tends to be limited to a region around the axis of the (old) streamer channel. As a result, the field intensity locally can reach the magnitudes required for the efficient RE generation [*Bakhov et al*., 2000].

Allowing for the ionization wave focusing, we shall model one part of the leader stepping process, namely, only forward propagation of the ionization wave, which velocity vector $\vec{v}_f$ is directed along the external electric force $-e\vec{E}_{\text{ext}}$. The negative leader is assumed to develop as illustrated in Figure 1 [*Babich et al*., 2014a, 2015]. According to *Bazelyan and Raizer* [2000, section 2.7], a scenario of the negative leader development is as follows. At the external boundary of the leader corona, a plasma formation develops, extending along the electric field vector. From both ends of this formation, streamers start in directions to and from the leader head. Further, the plasma formation with streamers transforms in the so-called space leader with negative

Table 1. RE Number Per Unit Streamer Length. Air, 1 atm, E_{ext} = 50 kV cm^{-1}, z_2 = 3 cm

$n_e^{i,ch,a}$, m^{-3}	t_{z_2}, ns	E_f, kV cm^{-1}	v_f, m s^{-1}	k_{re}, m^{-1}[a]	k_{re}^{MC}, m^{-1}
10^{10}	3.86	205	$1.3 \cdot 10^7$	$2 \cdot 10^4$	
10^{11}	3.80	267	$2 \cdot 10^7$	$5 \cdot 10^7$	$4.3 \cdot 10^7$
10^{12}	3.66	296	$2 \cdot 10^7$	$2 \cdot 10^9$	$2.3 \cdot 10^9$
10^{13}	3.50	286	$3 \cdot 10^7$	$9 \cdot 10^8$	$4.6 \cdot 10^8$
10^{14}	3.31	253	$3 \cdot 10^7$	$2 \cdot 10^7$	$2.8 \cdot 10^6$
10^{15}	3.14	204	$3 \cdot 10^7$	$3 \cdot 10^4$	

[a] *Babich et al*. [2014a, 2015].

and positive coronas. The positive head of the space leader with its corona moves toward the negative head of the main leader channel and, at contact, a united conducting channel is being formed with the potential of the old leader being transferred to the space leader [*Moss et al*., 2006; *Celestin and Pasko*, 2011]. The potential jump in the body of the space leader launches new ionization waves along the old streamer channels in the negative streamer corona ahead of the new leader head.

Proceeding from this scenario, *Babich et al*. [2014a, 2015] modeled the ionization wave propagation in a streamer channel using the diffusion-drift approximation of the fluid equations for free electrons and ions and showed that the intensity of the ionization wave field may reach magnitudes above 240 kV cm^{-1} [*Bakhov et al*., 2000] required for efficient generation of REs in the lower atmosphere. They further computed the magnitudes of the ionization wave speed v_f, space-time distributions of the electron concentration $n_e(z,\rho,t)$, and self-consistent field intensity $\vec{E}(z,\rho,t)$ in cylindrical set of coordinates $(\vec{z},\vec{\rho})$ with $\vec{z}$ and $\vec{\rho}$ directed accordingly against and orthogonal to the external field vector $\vec{E}_{ext}$. On the basis of the obtained results and with the use of a dependence of the RE production rate $\nu_{run}(E)$ on the field intensity [*Bakhov et al*., 2000], the RE production per unit streamer length was determined for different magnitudes of the initial electron concentration in the streamer channel. For an ionization wave propagating a distance z_2 - z_1 it is

$$k_{re} = \frac{N_{re}(t_{z_2}) - N_{re}(t_{z_1})}{z_2 - z_1}, \tag{1}$$

where

$$N_{re}(t) = \int_0^t \int_{V_{sim}} \nu_{run}\left(E\left(z,\rho,t'\right)\right) \cdot n_e\left(z,\rho,t'\right) \cdot dV \cdot dt'. \tag{2}$$

Here $N_{re}(t_z)$ is the number of REs at time t_z when the ionization wave front, defined as a position of the field maximum, has reached a point z; V_{sim} is the simulation domain volume [*Babich et al*., 2014a, 2015]. Values of v_f and k_{re} calculated with z_2 = 3.0 cm and z_2 - z_1 = 0.1 cm at the end of simulations in *Babich et al*. [2014a, 2015], when quasi-state electron concentration and field distributions were achieved, are presented in Table 1, where $n_e^{i,ch,a}$ is the *initial* electron concentration at the *channel* symmetry *axis*. It is seen, that v_f increases with $n_e^{i,ch,a}$ achieving a plateau. The dependence of k_{re} on $n_e^{i,ch,a}$ is more complicated: initially, k_{re} increases with $n_e^{i,ch,a}$ reaching a maximum magnitude at $n_e^{i,ch,a} = 10^{12}$ m^{-3}, and then decreases. This is explained as follows: at small $n_e^{i,ch,a}$, the field intensity and, consequently, the velocity v_f do not reach large magnitudes due to the streamer head radial expansion, and at large $n_e^{i,ch,a}$, the channel conductivity, which limits the field strength, grows faster than at lower $n_e^{i,ch,a}$ values.

The function $\nu_{run}(E)$, used in equation (2), was computed for a constant field [*Bakhov et al*., 2000], which is valid if the field intensity does not vary during electron trajectory simulations. However, at large v_f magnitudes, this is not the case. For instance, electrons, starting at the point where the field intensity is maximal, lag behind the maximum, if their initial velocity is less than the wave speed v_f, and enter a region with weaker field, whereas electrons, starting ahead of the field maximum, experience amplifying field because the wave overtakes them. This is not allowed in equation (2). It is necessary to take into account the displacement of electrons during their energizing to the runaway energy range because the field intensity gradient is very large in the vicinity of the field maximum.

Below, in section 2, the effect of a moving ionization wave on the production of REs is studied by Monte Carlo simulations. With this goal we use the electron concentration and field intensity spatial distributions [*Babich et al*., 2014a, 2015] obtained at the end of simulations, which invariable profiles we let to move with the given velocity v_f through a computational mesh. As a result of this motion, in each cell of the mesh, the electron concentration and field intensity vary. At each time step in each cell of the mesh, the RE numbers are computed as a number of electrons capable of overcoming the runaway threshold. In section 3, a scenario of the streamer propagation outside the old ionized channel allowing for the gas preionization by the REs ahead of the wave front is analyzed. Section 4 includes some further comments and conclusions.

2. The Effect of the Ionization Wave Speed on Runaway Electrons Production

We first analyze the most interesting case with the electron concentration $n_e^{i,\mathrm{ch},a} = 10^{12}$ m^{-3}, at which the k_{re} is at its maximum as calculated by *Babich et al*. [2014a, 2015] (see Table 1). With this goal, we execute 2-D Monte Carlo simulations and compute the generation rate of REs per unit length along the velocity direction of an ionization wave moving with a constant speed $v_f = 2\cdot 10^7$ m s^{-1} corresponding to $n_e^{i,\mathrm{ch},a} = 10^{12}$ m^{-3} (Table 1). The ionization wave is modeled as the spatial distributions of the electron concentration $n_e^{\mathrm{st}}(z,\rho)$ and field intensity $\overrightarrow{E}^{\mathrm{st}}(z,\rho)$, computed at the end of simulations (t = 3.6 ns) in *Babich et al*. [2014a, 2015]. The electron concentration and field intensity at each moment of time are then $n_e(z,\rho,t) = n_e^{\mathrm{st}}(z - v_f\cdot t,\rho)$ and $\overrightarrow{E}(z,\rho,t) = \overrightarrow{E}^{\mathrm{st}}(z - v_f\cdot t,\rho)$. The simulations are carried out with cell sizes $\Delta z = \Delta\rho = 10^{-5}$ m of the computation mesh and time step $\Delta t = 10^{-14}$ s.

Following the energy group technique [*Babich and Kutsyk*, 1995], we divide the electron ensemble in a "reservoir" of low-energy electrons, limited from above to some energy ε_1, and "high-energy" electrons with the energies $\varepsilon > \varepsilon_1$, the source of which is the "reservoir." We choose the ε_1 magnitude such that the concentration of low-energy electrons to be much higher than that of "high-energy" electrons, such that these are so few that do not affect the transport processes, the field magnitude, and ionization wave configuration. The preionization effect ahead of the ionization wave by electrons moving with a velocity higher than v_f will be discussed in the following section. The "high-energy" electrons produced in the ionization wave are further limited to the energy range [ε_1, $\varepsilon_{\mathrm{th}}$], where $\varepsilon_{\mathrm{th}}$ = 4 keV [*Bakhov et al*., 2000] is the runaway threshold. Note, limiting from below the energy to the magnitude ε_1, above which we carry out simulations, allows us to limit the number of trajectories to be simulated. We do this by using the electron production rate $\nu_1(\varepsilon_1, E)$ computed beforehand with the same Monte Carlo code.

The ε_1 magnitude is to be chosen to compromise between the accuracy requirements and limitations of a computer capacity limiting the number of simulated trajectories. Therefore, to check whether reasonably chosen ε_1 magnitude will affect the results, we carried out test Monte Carlo simulations of $N_{\mathrm{sim}} = 10^6$ electron trajectories in the field with the constant intensity E = 270 kV cm^{-1} for two ε_1 magnitudes: 100 and 200 eV. A number of physical electrons $N_{\mathrm{th}}(\varepsilon_1, \varepsilon_{\mathrm{th}})$, crossing the runaway threshold $\varepsilon_{\mathrm{th}}$ = 4 keV [*Bakhov et al*., 2000], is connected with an initial number of low-energy electrons $N_e^{(0)}(\varepsilon_1)$, crossing the border ε_1, and relative number of successful simulated trajectories $N_{\mathrm{th,sim}}(\varepsilon_1, \varepsilon_{\mathrm{th}})/N_{\mathrm{sim}}$ as follows:

$$N_{\mathrm{th}}(\varepsilon_1, \varepsilon_{\mathrm{th}}) = N_e^{(0)}(\varepsilon_1)\times\frac{N_{\mathrm{th,sim}}(\varepsilon_1, \varepsilon_{\mathrm{th}})}{N_{\mathrm{sim}}} \sim \nu_1(\varepsilon_1)\times\frac{N_{\mathrm{th,sim}}(\varepsilon_1, \varepsilon_{\mathrm{th}})}{N_{\mathrm{sim}}}, \tag{3}$$

where ν_1 is the rate with which the low-energy electrons cross the border ε_1.

With the magnitudes of the rate $\nu_1(\varepsilon_1 = 200$ eV) and $\nu_1(\varepsilon_1 = 100$ eV), available in *Bakhov et al*. [2000], and computed numbers $N_{\mathrm{th,sim}}(\varepsilon_1 = 200$ eV, $\varepsilon_{\mathrm{th}})$ and $N_{\mathrm{th,sim}}(\varepsilon_1 = 100$ eV, $\varepsilon_{\mathrm{th}})$, a ratio of $N_{\mathrm{th}}(\varepsilon_1, \varepsilon_{\mathrm{th}})$ for the above ε_1 magnitudes

$$\frac{N_{\mathrm{th}}(\varepsilon_1 = 200\ \mathrm{eV},\ \varepsilon_{\mathrm{th}})}{N_{\mathrm{th}}(\varepsilon_1 = 100\ \mathrm{eV},\ \varepsilon_{\mathrm{th}})} = \frac{\nu_1(\varepsilon_1 = 200\ \mathrm{eV})}{\nu_1(\varepsilon_1 = 100\ \mathrm{eV})}\times\frac{N_{\mathrm{th,sim}}(\varepsilon_1 = 200\ \mathrm{eV},\ \varepsilon_{\mathrm{th}})}{N_{\mathrm{th,sim}}(\varepsilon_1 = 100\ \mathrm{eV},\ \varepsilon_{\mathrm{th}})} \tag{4}$$

is close to the unity, meaning that the number $N_{\mathrm{th}}(\varepsilon_1, \varepsilon_{\mathrm{th}})$ of runaway electrons rather weakly depends on the choice of ε_1 magnitude within a reasonable range. This could be expected because with ε_1 = 100 eV, a number of successful trajectories is lower than with ε_1 = 200 eV, but $\nu_1(\varepsilon_1 = 100$ eV) is higher than $\nu_1(\varepsilon_1 = 200$ eV).

In the subsequent Monte Carlo simulations with the field profile as in *Babich et al.* [2014a, 2015], we let ε_1 = 200 eV due to larger number of successful trajectories and smaller computation time. Were we to carry out the simulations with ε_1 = 100 eV, rather than with ε_1 = 200 eV, the difference would only be the additional trajectory section in the range from 100 to 200 eV. The energizing time from 100 to 200 eV is on the order of the difference in the time lag $t_d(\varepsilon_1)$ required to cross the border ε_1 [*Bakhov et al.*, 2000] $\Delta t_d = t_d(200\ \text{eV}) - t_d(100\ \text{eV}) < 10^{-12}$ s, during which the field does not significantly vary and the electron displacement is less than the cell size.

The generation rate of the "high-energy" electrons per unit volume is computed by a formula similar to the integrand in equation (2):

$$S_1(z,\rho,t,\varepsilon_1) = \nu_1(E(z,\rho,t),\varepsilon_1)\cdot n_e(z,\rho,t). \tag{5}$$

To compute the ν_1 dependence on the field intensity, we use the approach that *Bakhov et al.* [2000] used for computing the runaway rate $\nu_{\text{run}}(E)$ and the same set of elementary cross sections, taking into account elastic scattering, excitation of electronic shells, and impact ionization. As the rate $S_1(z,\rho,t,\varepsilon_1)$ in formula (5) depends on the local electric field and electron concentration, it is necessary that the locality principle be satisfied; i.e., the kinetics of low-energy electrons be governed by the local field. In the field with the intensity $E > 200$ kV cm^{-1} during a time lag $t_d \approx 2\cdot 10^{-12}$ s required to cross the border ε_1 = 200 eV (electron velocity $v_e = 0.8\cdot 10^7$ m s^{-1}) [*Bakhov et al.*, 2000], low-energy electron moves for a distance $eEt_d^2/2m_e$ of $3.5\cdot 10^{-6}$ m, which is less than the cell sizes $\Delta z = \Delta\rho = 10^{-5}$ m of the computational mesh. Since the electron velocity v_e is of the order of the wave speed v_f and the vector $\vec{v}_f$ is directed along the external electric force $-e\vec{E}_{\text{ext}}$, the electron concentration and field intensity vary insignificantly with time. The chosen time step $\Delta t = 10^{-14}$ s is significantly less than $t_d \approx 2\cdot 10^{-12}$, which, in its turn, is significantly less than the characteristic time of the field variation $\tau_E \approx \lambda_E/v_f > 5\cdot 10^{-11}$ s, where λ_E is the width of the field wave profile. Here we use $\lambda_E = (d\ln E/dz)^{-1} \approx 5\cdot 10^{-4}$ m for the strongest part of the field profile from [*Babich et al.*, 2014a; *Babich et al.*, 2015], where $E \geq 240$ kV cm^{-1} required for the electron runaway. Naturally, the total profile width and, consequently, τ_E, are larger. Thus, the locality principle is satisfied.

Because we use an ionization wave propagating without attenuation or dispersion, i.e., with invariable (in the reference frame connected with the wave) electron concentration and field profiles and magnitudes, all disk layers with a thickness equal to the step $\Delta z = 10^{-5}$ of the computational mesh operate as sources of electrons with the energy ε_1 during the wave passage through each of them. They produce the same number of "high-energy" electrons, although with some time delay according to the equation $S_1(z_1,\rho,t) = S_1(z_2,\rho,t-(z_2-z_1)/v_f)$, where z_1 and z_2 are the coordinates of the disks. In view of our goal to compute the RE numbers per unit length, it is sufficient to execute the simulations of electrons with the initial energy ε_1 generated only in a single disk layer of thickness Δz. The simulations do not account for the preionization due to REs.

We place the disk layer in the vicinity of the coordinate z_0 far ahead of the coordinate $z_{\max}$ of the field maximum ($z_0 - z_{\max} \approx$ 0.5–1 cm at the start of the computation; Figure 2). In each cell of the mesh with a volume $\Delta V = 2\pi\rho\Delta\rho\Delta z$ in each time interval $[t, t+\Delta t_{\text{gen}}]$, an ensemble, containing $\Delta N_1 = S_1(z,\rho,t)\cdot 2\pi\rho\Delta\rho\Delta z\cdot\Delta t_{\text{gen}}$ electrons with the energy ε_1, is generated. We use $\Delta t_{\text{gen}} = 10^{-13}$ s and simulate the further ensemble behavior with a time step of $\Delta t \approx 10^{-14}$ s by a trajectory of one test electron with initial energy ε_1 and weighted with ΔN_1. The technique of trajectory simulations follows *Bakhov et al.* [2000]. The simulations are carried out until the test electron achieves the threshold ε_{th} or decelerates down to the range $\varepsilon \leq 1$ eV. In the first case the energy ε_{th} is prescribed to all ΔN_1 electrons; this is statistically reasonable owing to small size and large number of the cells, small Δt_{gen}, and accordingly, large number of simulated trajectories (hundreds of thousands of trajectories are simulated simultaneously). After each time step Δt_{gen}, an additional ensemble of new "high-energy" electrons in each cell of the layer is generated, which trajectories are simulated as described above. The sought RE numbers are computed, summing the weights of all test electrons achieving the threshold ε_{th}: $N_{\text{re}} = \sum_i \Delta N_1^i(\varepsilon_{\text{th}})$. Sensitivity trial computations with twofold decrease of Δt_{gen} (twofold decrease in ΔN_1) give essentially the same RE number. Note, unlike the fluid calculations by *Babich et al.* [2014a, 2015], the Monte Carlo simulations account for the spatial and temporal changes in the field conditioned to the wave motion.

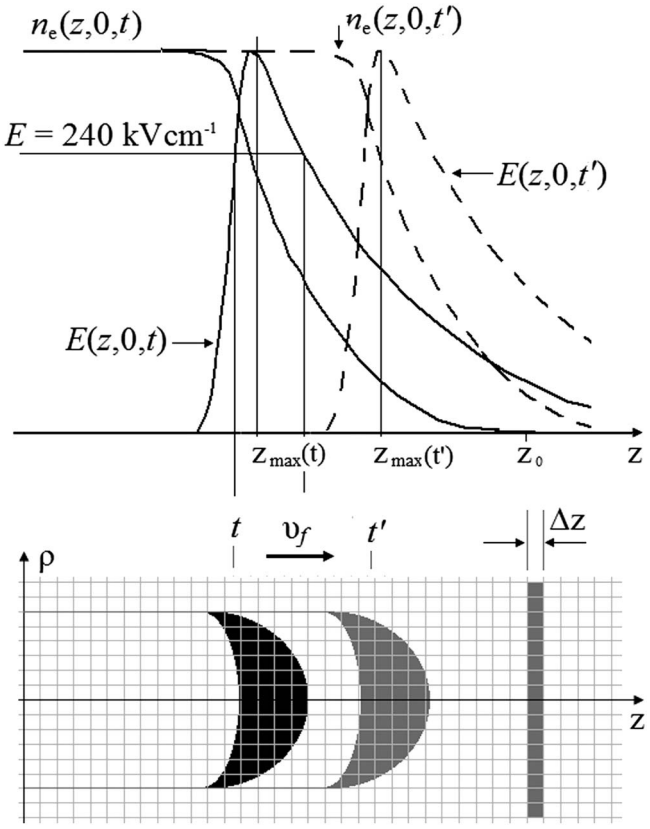

Figure 2. Scheme of the RE simulations. (top) Electric field and electron concentration profiles at the moment of time t. The field scale is of $\lambda_E = 5 \cdot 10^{-4}$ m in the region with $E \geq 240$ kV cm^{-1} required for the generation of REs, $\upsilon_f < < \lambda_E/t_d < 5 \cdot 10^7$ m s^{-1}; $t_d \approx 10^{-11}$ s is a delay time required for the production of the first RE [*Bakhov et al.*, 2000]. (bottom) A source of electrons with the (right) energy ε_1 localized in the one-step layer Δz at the same moment of time t and the (left) RE volumetric source for two moments of time t and t'.

Unlike equation (1), the RE number per unit length born by the ionization wave moving with a set constant velocity υ_f is calculated as follows:

$$k_{re}^{MC}(z_0, \upsilon_f) = \frac{N_{re}}{\Delta z} = \frac{1}{\Delta z}\int_0^{t_{max}} dN_{re}(z_0, \upsilon_f, t), \quad (6)$$

where $dN_{re}(z_0, t)$ is the number of high-energy electrons created in the layer $[z_0, z_0 + \Delta z]$ and reached the runaway threshold ε_{th} within the time range $[t, t + dt]$ and t_{max} is the time required to simulate the ionization wave passage through the layer $[z_0, z_0 + \Delta z]$. Using equation (6), instead of (1) allows reducing a number of simulated electron trajectories and increasing the calculation accuracy.

Simulations with $n_e^{i,ch,a} = 10^{12}$ m^{-3} and $\upsilon_f = 2 \cdot 10^7$ m s^{-1} give the RE number per unit length $k_{re}^{MC} = 2.3 \cdot 10^9$ m^{-1}, which is comparable to $k_{re} = 2 \cdot 10^9$ m^{-1} [*Babich et al.*, 2014a; *Babich et al.*, 2015] (Table 1). Hence, within the model and simulation accuracy, it is not necessary in this case to account for the field variations during the electron energizing. The wave field does not undergo significant variations during time t_{max}, which is orders of the magnitude less than the simulation time in *Babich et al.* [2014a, 2015].

To determine the validity range in υ_f of the rate k_{re} estimated in *Babich et al.* [2014a, 2015], we carry out simulations with different υ_f magnitudes using the same distributions of the electron concentration $n_e^{st}(z - \upsilon_f \cdot t, \rho)$ and field intensity $\vec{E}^{st}(z - \upsilon_f \cdot t, \rho)$ as earlier, again keeping the υ_f magnitude constant. The obtained k_{re}^{MC} as a function of υ_f is displayed in Figure 3 along with the following analytical evaluation:

$$k_{re}(z_0) = \frac{1}{\Delta z}\int_0^{t_{max}} dN_{re}(z_0, t), \quad (7)$$

where

$$dN_{re}(z_0, t) = dt \Delta z \int_0^{\rho_{sim}} \nu_{run}(E(z_0, \rho, t)) \cdot n_e(z_0, \rho, t) 2\,\pi\,\rho d\,\rho. \quad (8)$$

Here the radial size of the computation area used, $\rho_{sim} = 6$ mm, is the same as the in *Babich et al.* [2014a, 2015] and $\nu_{run}(E)$ is taken from *Bakhov et al.* [2000].

It is seen that for $\upsilon_f < 2 \cdot 10^7$ m s^{-1}, the estimations and results of Monte Carlo simulations are rather close, whereas at $\upsilon_f > 3 \cdot 10^7$ m s^{-1} equation (7) with integrand (8) strongly overestimates the RE numbers. The reason is that equation (8) is valid, provided the field varies weakly during the delay time $t_d \approx 10^{-11}$ s required for the production of the first RE with the energy $\varepsilon_{th} = 4$ keV [*Bakhov et al.*, 2000], i.e., $\tau_E \approx \lambda_E/\upsilon_f > > t_d$, where τ_E and λ_E are the wave temporal and spatial scales. For $\lambda_E = (d \ln E/dz)^{-1} \approx 5 \cdot 10^{-4}$ m in the region near the

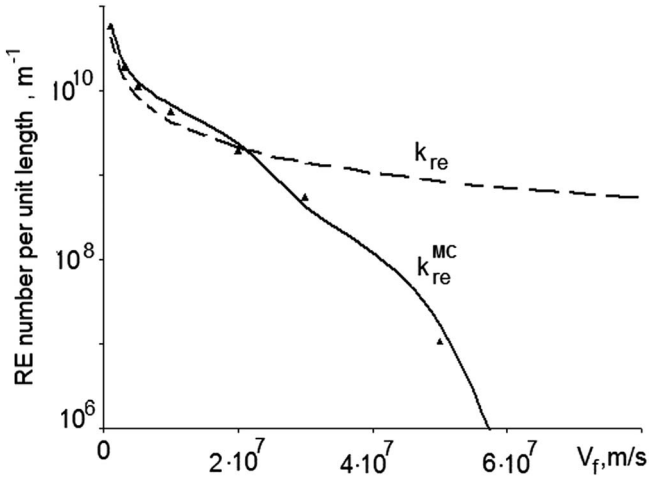

Figure 3. A dependence of the RE number per unit streamer length on the ionization wave velocity at $n_e^{i,ch,a} = 10^{12}$ m^{-3}. Estimations using equation (8) (dotted line), simulations using a source of electrons with the energy ε_1 localized in the layer with thickness Δz (solid line), and simulations with the RE volumetric generation (markers).

strongest part of the wave field, where $E \geq 240$ kV cm^{-1} [*Babich et al.*, 2014a, 2015], we obtain an inequality $v_f << \lambda_E/t_d < 5 \cdot 10^7$ m s^{-1}, which is consistent with our Monte Carlo results.

The rate k_{re}^{MC} depends strongly on the wave velocity decreasing by orders of the magnitude with only a threefold increase in v_f. The reason is that the velocities of electrons in the range $[\varepsilon_1, \varepsilon_{th}]$ are within the range $[0.75, 3.75] \cdot 10^7$ m s^{-1}; hence, for $v_f \geq 3.75 \cdot 10^7$ m s^{-1}, electrons lag behind the high-field region such that the runaway probability strongly decreases.

Note, in the fluid simulations the field and electron concentration distributions change with time; in particular, the field profile widens and amplitude increases [*Babich et al.*, 2014a, 2015]. Here we use the same distributions from *Babich et al.* [2014a, 2015], and our simulations are therefore not fully self-consistent. This, however, does not affect the results because the changes in the distributions due to the wave motion in the time t_{max}, considered are small. For instance, $t_{max} \sim z_0 - z_{max}/v_f \sim 5 \cdot 10^{-3}$ m/$(2-6) \cdot 10^7$ m s^{-1} $\approx (2.5-1) \cdot 10^{-10}$ s is much less than the characteristic time of the field variation in Figure 4 in *Babich et al.* [2015], which is in the nanosecond range.

The values of k_{re}^{MC}, computed for different $n_e^{i,ch,a}$ magnitudes, are shown in the last column of Table 1. They vary from $\sim 3 \cdot 10^6$ to $\sim 2 \cdot 10^9$ m^{-1}. A comparison with k_{re} magnitudes computed in *Babich et al.* [2014a, 2015] and presented in Table 1 gives the same validity range of the v_f estimations.

From the simulation results we find that the electrons with the energy ε_1, starting when the field intensity in the disk layer Δz is $E \geq 240$ kV cm^{-1}, contribute most to the RE generation. Owing to this, we are able to compute the RE numbers by simulating trajectories of "high-energy" electrons starting not only in the space domain limited to one Δz-thick layer of the computational mesh but also trajectories starting in all cells of the mesh, in which at the moment of the trajectory start, the field strength exceeds 240 kV cm^{-1}. In such a case we simulate the moving volumetric source of electrons with the energy ε_1 giving start to new trajectories (Figure 2), unlike to the case with immobile source in the thin Δz layer. This "volumetric" k_{re}^{MC}, computed from the simulations and using equation (1), is shown in Figure 3 as a function of v_f. The difference from the k_{re}^{MC}, computed with the a single thin disk layer ($\Delta z = 10^{-5}$ m) and considering the full range of fields in that layer, does not exceed 10%, although much fewer trajectories, ~20,000, were simulated at each moment of time.

3. The Effect on the Streamer Propagation of the Air Preionization by Runaway Electrons

We now show that even with the k_{re} values far away from the maximal set magnitudes, the additional ionization by RE beam ahead of the wave can exceed the initial electron concentration $n_e^{i,ch,a}$. Figure 4 shows radial distribution of the REs concentration

$$f_{re}(\rho) = n_{re}(\rho, \varepsilon_{th}) / \int_0^{\rho_{sim}} n_{re}(\rho, \varepsilon_{th}) 2\,\pi\,\rho d\,\rho \tag{9}$$

and the initial concentration distribution of low-energy electrons in the old streamer channel

$$f_e(\rho) = n_e^{ch}(\rho) / \int_0^{\rho_{sim}} n_e^{ch}(\rho) 2\,\pi\,\rho d\,\rho, \tag{10}$$

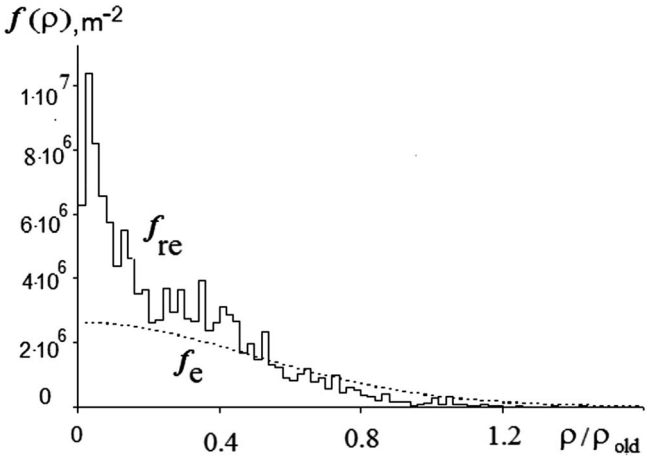

Figure 4. Radial distributions of runaway (solid line) and low-energy (dotted line) electrons in the old streamer channel.

where the ρ_{sim} = 6 mm as in *Babich et al.* [2014a, 2015].

It is seen that REs are concentrated close to the channel axis. The REs, born at small distances away from the ionization wave front, contribute most of all in the volumetric ionization, whereas the contribution of REs distant from the wave front is much lower due to the RE beam expansion and chaotization of the RE velocity vectors. Hence, the characteristic radial size of the RE beam near the ionization wave front does not exceed that of the old streamer channel $\rho_{old} \approx 5 \cdot 10^{-4}$ m [*Babich et al.*, 2014a, 2015]. We next let the radial size of the RE beam be equal to this magnitude and consider the REs, born, for instance, along the length $l = 10^{-3}$ m passed by the wave front. Then, the RE contribution to the channel ionization can be estimated as

$$\Delta n_e^{re} = \left(k_{re} \cdot l \cdot N_{e,1}\right)/\pi\rho_{old}^2, \tag{11}$$

where the number of low-energy electrons per unit length $N_{e,1}$, produced by an electron with the threshold energy ε_{th} = 4 keV, can be estimated as the ratio of the specific energy losses $L(\varepsilon_{th})$ to the ionization energy cost in air $\Delta\varepsilon$. Using for $L(\varepsilon_{th})$, Bethe's formula for electron energy losses per unit length [*Bethe and Ashkin*, 1953] at atmospheric number density of neutrals and $\Delta\varepsilon$ = 34 eV [cf. *Dwyer and Babich*, 2011, and citations therein], we obtain $N_{e,1} \approx 10^5 m^{-1}$.

Even with the overestimated RE beam radial size $\rho_{old} \approx 5 \cdot 10^{-4}$ m and underestimated RE number $k_{re} \cdot l = 10^4$, computed using rather low $k_{re} = 10^7$ m^{-1} (Figure 3), we get $\Delta n_e^{re} \approx 10^{15} m^{-3}$, which exceeds the maximal $n_e^{ch,a,i}$ magnitude in Table 1. Hence, the ionization wave propagation is determined by the air ionization by the REs ahead of the wave front instead of being governed by the old channel plasma parameters. Thus, the preionization anisotropy ahead of the ionization wave, required according to *Babich et al.* [2014a, 2015] to focus the wave in order to reach the field intensity magnitudes of ≥240 kV cm^{-1} that allow efficient RE generation, can be provided with a RE beam itself once the beam has been created. This suggests that the process is self-sustained.

The old streamer channel provides the anisotropic preionization only at the start of new streamer before appearing even rather small number of REs but sufficient for producing the preionization with $\Delta n_e^{re} > n_e^{ch,a,i}$. Further, the streamer can propagate independently and not necessarily along the old channel. Naturally, direct measurements of local fields as strong as 240 kV cm^{-1} are absent. However, as pointed out in the introduction, the observations of bremsstrahlung X- and γ-rays, correlated with electromagnetic pulses of leader steps [e.g., *Dwyer et al.*, 2004, 2005, 2012b], suggest that high-energy REs are generated, which, in turn, is evidence that the electric field intensity in the stepping process is increased to at least 240 kV cm^{-1} in a region close to the leader tip.

REs, even in small numbers, say 10, create per unit length a rather large number of seed electrons ($\sim 10 \cdot N_{e,1} \approx 10^6$ m^{-1}). It is almost the same as the number of seed electrons per unit length of the old streamer channel $n_e^{ch,a,i} \cdot \pi\rho_{old}^2 \approx 10^{12}$ m$^{-3} \times \pi \cdot (5 \cdot 10^{-4}$ m$)^2 \sim 0.8 \cdot 10^6$ m^{-1}, which is sufficient for the ionization wave focusing. Hence, the streamer, once formed, may propagate in a casual direction as a result of the field fluctuations, as small RE numbers (~10) are generated. As a result, new channels may be formed, in which the current grows and charge is accumulated, strengthening the local field and thus promoting the further channel growth. In this process, the new channel can be narrower than that of the old streamer.

To prove the idea of the self-consistent streamer development in the RE mode, simulations with self-consistent description of the RE kinetics and the ionization wave propagation are planned. Such

simulations can be executed using the group approach developed by *Babich and Kutsyk* [1995], according to which the electron assembly is divided into three energy groups: low-energy electrons, intermediate-energy electrons, and REs in the energy range $\varepsilon > \varepsilon_{th}$. According to this approach, the low-energy electrons are described by the kinetic equation; the probability for electrons "flowing out" off the low-energy range and into the RE range is calculated with ignoring elastic collisions; the RE kinetics is described by the fluid equation in the diffusion-drift approximation.

Now an improved group approach is available. For describing the kinetics of low-energy ($\varepsilon < \varepsilon_1$) electrons in the electric field, it is sufficient to use the numerical code using the diffusion-drift approximation for the fluid equations, similar to that developed by *Babich et al*. [2014a, 2015]. To simulate the electron kinetics in the intermediate energy range $[\varepsilon_1, \varepsilon_{th}]$, it is reasonable to use the approach described above. The RE kinetics in the energy range $\varepsilon > \varepsilon_{th}$ can be simulated by means of a simplified Monte Carlo code [*Lehtinen et al*., 1999; *Babich et al*., 1998, 2001a, 2001b], in which a model of continuous energy losses and Rutherford's equation with shielding for the angular scattering are used or by means of the group equations for the electron distribution function moments [*Babich and Kudryavtseva*, 2007; *Babich and Bochkov*, 2011].

4. Conclusions

In the framework of the problem of high-energy REs and bremsstrahlung generation by leaders of the long spark discharges, including those of the natural lightning, we have analyzed the evaluations of the RE numbers per unit streamer length carried out by *Babich et al*. [2014a, 2015] on the basis of results of numerical simulations of the streamer development using diffusion-drift approach for the fluid equations. By means of Monte Carlo simulations, we show that the evaluations in *Babich et al*. [2014a, 2015] are rather accurate at the ionization wave velocities in the range $v_f < 2 \cdot 10^7$ m s^{-1} , but at higher velocities, results of and evaluations manifold differ. The computed RE numbers per unit streamer length vary in the range from about $3 \cdot 10^6$ to $2 \cdot 10^9$ m^{-1}, depending on the v_f magnitude.

In this paper we consider discharges in the open atmosphere in rather weak external electric fields with the intensity many-fold below the maximum of the electron drag force $F_{max} \approx 270$ kV cm^{-1} [*Nguyen et al*., 2008; *Rahman et al*., 2008; *March and Montanya*, 2010; *Kochkin et al*., 2012, 2014, 2015; *Ostgaard et al*., 2016; *Agafonov et al*., 2013], when the total charge of REs only constitutes insignificant portion of the electricity accumulated in the source: thundercloud (lightning) or capacitor bank (laboratory long spark), unlike the discharges in superstrong external fields with the intensity close to or even higher than F_{max} [e.g., *Babich et al*., 1990, 2014b; *Babich*, 2003, chapter 5, 2005; *Tarasenko and Yakovlenko*, 2004; *Yalandin et al*., 2011, 2012, and citations therein]. The ionization waves in discharges developing in superstrong fields propagate with speeds close to that of light in free space, and it is recognized that such discharges develop self-consistently with a production of large numbers of high-energy REs, which preionize a gas ahead of the ionization wave front [*Babich et al*., 1990; *Babich*, 2003, section 4.2, 2015; *Yalandin et al*., 2011, 2012].

In this paper, we show that even at rather low ionization wave speed, $v_f < 2 \cdot 10^7$ m s^{-1} , the concentration of low-energy electrons produced by small numbers of REs in front of the streamer can significantly exceed the initial concentration of low-energy seed electrons in the old streamer channel. Hence, an adequate mechanism of the streamer propagation in lightning and long laboratory spark discharges also is self-consistent with the RE generation. The above analyses were executed using the electron concentration and field intensity profiles from *Babich et al*. [2014a, 2015] computed at atmospheric air density. To support a propagation of lightning leader/streamer channels, the process of the RE generation should work in the span of altitudes typical for the lightning discharges, i.e., from ground level to tens of kilometers. All results obtained at the ground level can be generalized to streamers at other altitudes (air densities) of interest using similarity laws, according to which the streamer spatial dimensions (such as a length and tip width) and electric field scale with the air density N as ~1/N and ~N, respectively [*Pasko et al*., 1998; *Liu and Pasko*, 2004; *Moss et al*., 2006]. As a result, numbers of REs and maximum energy they gain in the streamer tip remain the same for similar streamers at different air densities (assuming constant gas temperature). Therefore, the effect of REs on the propagation of lightning leader/streamer channels is almost the same at different altitudes.

We considered the electron runaway in strong electric fields of the heads of streamers constituting the leader corona. However, electron energizing depends on the *E*/*N*, not simply on *E*. Therefore, there is a chance that electrons can be energized in the hot leader channel. Really, due to the heated gas expansion, the air density in the channel can be reduced to a level, at which the *E*/*N* is increased up to a magnitude sufficiently high for producing high-energy REs.

The simulations of the runaway process carried out in this paper are not self-consistent because the moving distributions of electron concentration and the field strength do not vary self-consistently with the RE generation. But the Monte Carlo code developed in this work can be used in the streamer model with self-consistent generation of high-energy REs. This methodology will be applied in our continued work.

Acknowledgments
The VNIIEF coauthors express the deepest gratitude to C. Haldoupis, who, in cooperation with T. Neubert, has been an international collaborator in the completed ISTC project 3993-2010 and to N. Crosby, S. Cummer, A. van Deursen, J.R. Dwyer, R. Roussel-Dupre, D. Smith, T. Torii, and E. Williams for their support of the project proposal. They thank R.A. Roussel-Dupre and E.M.D. Symbalisty for the long-term collaboration, the continuation of which is this paper. The authors would like to thank the reviewers whose invaluable comments have allowed significant improvement of this paper. AGU data policy is addressed. The readers can access the data that support or underlie the conclusions presented in this manuscript in the cited references. No new data or models are used.

References

Agafonov, A. V., A. V. Bagulya, O. D. Dalkarov, M. A. Negodaev, A. V. Oginov, A. S. Rusetskiy, V. A. Ryabov, and K. V. Shpakov (2013), Observation of neutron bursts produced by laboratory high-voltage atmospheric discharge, *PRL*, *111*, 115003.

Babich, L. P. (2003), *High-Energy Phenomena in Electric Discharges in Dense Gases: Theory, Experiment and Natural Phenomena*, Futurepast Inc., Arlington.

Babich, L. P. (2005), Analysis of a new electron-runaway mechanism and record-high runaway-electron currents achieved in dense-gas discharges, *Phys.-Uspekhi*, *48*, 1015–1037, doi:10.1070/PU2005v048n10ABEH002805.

Babich, L. P., and E. I. Bochkov (2011), Deterministic methods for numerical simulation of high-energy runaway electron avalanches, *JETP*, *112*(3), 494–503, doi:10.1134/S1063776111020014.

Babich, L. P., and M. L. Kudryavtseva (2007), Group equations for moments of the relativistic electron distribution function in a cold gas of neutral atomic particles in an external electric field, *JETP*, *104*(5), 704–714, doi:10.1134/S1063776107050044.

Babich, L. P., and I. M. Kutsyk (1995), Numerical simulation of a nanosecond discharge in helium at atmospheric pressure, developing in the regime of runaway of electrons, *High Temp.*, *33*(2), 190–197.

Babich, L. P., T. V. Lo¨iko, and V. A. Tsukerman (1990), High-voltage nanosecond discharge in a dense gas at a high overvoltage with runaway electrons, *Soviet Phys. Uspekhi*, *33*, 521–540.

Babich, L. P., I. M. Kutsyk, A. Y. Kudryavtsev, and E. N. Donskoy (1998), New data on space and time scales of relativistic runaway electron avalanche for thunderstorm environment: Monte Carlo calculations, *Phys. Lett. A*, *245*, 460–470.

Babich, L. P., E. N. Donskoy, R. I. Il'kaev, A. Y. Kudryavtsev, I. M. Kutsyk, and B. N. Shamraev (2001a), The avalanche-development rate for runaway relativistic electrons under normal atmospheric conditions, *Dokl. Phys.*, *379*(5), 536.

Babich, L. P., E. N. Donskoy, I. M. Kutsyk, A. Y. Kudryavtsev, R. A. Roussel-Dupre, B. N. Shamraev, and E. M. D. Symbalisty (2001b), Comparison of relativistic runaway electron avalanche rates obtained from Monte Carlo simulations and from kinetic equation solution, *IEEE Trans. on Plasma Sci.*, *29*(3), 430–438.

Babich, L. P., E. I. Bochkov, and I. M. Kutsyk (2014a), Mechanism of generation of runaway electrons in a lightning leader, *JETP Lett.*, *99*(7), 386–390.

Babich, L. P., T. V. Loiko, and A. V. Rodigin (2014b), The first observations of Cherenkov's radiation of runaway electrons produced by discharge in dense gas, *IEEE Trans. Plasma Sci.*, *42*, 948–952, doi:10.1109/TPS.2014.23085292014b.

Babich, L. P., E. I. Bochkov, I. M. Kutsyk, T. Neubert, and O. Charnion (2015), A model for electric field enhancement in lightning leader tips to levels allowing X- and γ-ray emissions, *J. Geophys. Res. Space Physics*, *120*, 5087–5100, doi:10.1002/2014JA020923.

Bakhov, K. I., L. P. Babich, and I. M. Kutsyk (2000), Temporal characteristics of runaway electrons in electron—Neutral collision dominated plasma of dense gases. Monte Carlo calculations, *IEEE Trans. on Plasma Sci.*, *28*(4), 1254.

Bazelyan, E. M., and Y. P. Raizer (1998), *Spark Discharge*, CRC Press, Boca Raton, Fla.

Bazelyan, E. M., and Y. P. Raizer (2000) *Lightning Physics and Lightning Protection*, IOP, Bristol, England.

Bethe, H., and U. Ashkin (1953), Passage of radiation through matter, in *Experimental Nuclear Physics*, vol. 1, Part 2, edited by E. Segre, pp. 166–357, Wiley, New York.

Biagi, C. J., M. A. Uman, J. D. Hill, D. M. Jordan, V. A. Rakov, and J. Dwyer (2010), Observations of stepping mechanisms in a rocket-and-wire triggered lightning flash, *J. Geophys. Res.*, *115*, D23215, doi:10.1029/2010JD014616.

Biagi, C. J., M. A. Uman, J. D. Hill, and D. M. Jordan (2011), Observations of the initial, upward-propagating, positive leader steps in a rocket-and-wire triggered lightning discharge, *Geophys. Res. Lett.*, *38*, L24809, doi:10.1029/2011GL049944.

Biagi, C. J., M. A. Uman, J. D. Hill, and D. M. Jordan (2014), Negative leader step mechanisms observed in altitude triggered lightning, *J. Geophys. Res. Atmos.*, *119*, 8160–8168, doi:10.1002/2013JD020281.

Celestin, S., and V. P. Pasko (2011), Energy and fluxes of thermal runaway electrons produced by exponential growth of streamers during the stepping of lightning leaders and in transient luminous events, *J. Geophys. Res.*, *116*, A03315, doi:10.1029/2010JA01626.

Dwyer, J. R. (2004), Implications of X-ray emission from lightning, *Geophys. Res. Lett.*, *31*, L12102, doi:10.1029/2004GL019795.

Dwyer, J. R., and L. P. Babich (2011), Low-energy electron production by relativistic runaway electron avalanches in air, *J. Geophys. Res.*, *116*, A09301, doi:10.1029/2011JA016494.

Dwyer, J. R., et al. (2004), A ground level gamma-ray burst observed in association with rocket-triggered lightning, *Geophys. Res. Lett.*, *31*, L05119, doi:10.1029/2003GL018771.

Dwyer, J. R., et al. (2005), X-ray bursts associated with leader steps in cloud-to-ground lightning, *Geophys. Res. Lett.*, *32*, L01803, doi:10.1029/2004GL021782.

Dwyer, J. R., Z. Saleh, H. K. Rassoul, D. Concha, M. Rahman, V. Cooray, J. Jerauld, M. A. Uman, and V. A. Rakov (2008), A study of X-ray emission from laboratory sparks in air at atmospheric pressure, *J. Geophys. Res.*, *113*, D23207, doi:10.1029/2008JD010315.

Dwyer, J. R., D. M. Smith, and S. A. Cummer (2012a), High-energy atmospheric physics: Terrestrial gamma-ray flashes and related phenomena, *Space Sci. Rev.*, *173*, 133–196, doi:10.1007/s11214-012-9894-0.

Dwyer, J. R., M. M. Schaal, E. S. Cramer, S. Arabshahi, N. Liu, H. K. Rassoul, J. D. Hill, D. M. Jordan, and M. A. Uman (2012b), Observation of a gamma-ray at ground level in association with a cloud-to-ground lightning return stroke, *J. Geophys. Res.*, *117*, A10303, doi:10.1029/2012JA017810.

Gorin, B. N., V. I. Levitov, and A. V. Shkilev (1976), Some principles of leader discharge of air gaps with a strong non-uniform field, in gas discharges, *IEE Conf. Publ.*, *143*, 274–278.

Kochkin, P. O., C. V. Nguyen, A. P. J. van Deursen, and U. Ebert (2012), Experimental study of hard X-rays emitted from metre-scale positive discharges in air, *J. Phys. D: Appl. Phys.*, *45*, 425202, doi:10.1088/0022-3727/45/42/425202.

Kochkin, P. O., A. P. J. van Deursen, and U. Ebert (2014), Experimental study of the spatio-temporal development of meter-scale negative discharge in air, *J. Phys. D: Appl. Phys.*, *47*, 145203, doi:10.1088/0022-3727/47/14/145203.

Kochkin, P. O., A. P. J. van Deursen, and U. Ebert (2015), Experimental study on hard X-rays emitted from meter-scale negative discharges in air, *J. Phys. D: Appl. Phys.*, *48*, 025205, doi:10.1088/0022-3727/48/2/025205.

Lehtinen, N. G., T. F. Bell, and U. S. Inan (1999), Monte Carlo simulation of runaway MeV air breakdown with application to red sprites and terrestrial gamma ray flashes, *J. Geophys. Res.*, *104*, 24,699–24,712.

Liu, N., and V. P. Pasko (2004), Effects of photoionization on propagation and branching of positive and negative streamers in sprites, *J. Geophys. Res.*, *109*, A04301, doi:10.1029/2003JA010064.

March, V., and J. Montanya (2010), Influence of the voltage-time derivative in X-ray emission from laboratory sparks, *Geophys. Res. Lett.*, *37*, L19801, doi:10.1029/2010GL044543.

Moss, G. D., V. P. Pasko, N. Liu, and G. Veronis (2006), Monte Carlo model for analysis of thermal runaway electrons in streamer tips in transient luminous events and streamer zones of lightning leaders, *J. Geophys. Res.*, *111*, A02307, doi:10.1029/2005JA011350.

Nguyen, C. V., A. P. J. van Deursen, and U. Ebert (2008), Multiple X-ray bursts from long discharges in air, *Phys. D: Appl. Phys.*, *41*, 234012, doi:10.1088/0022-3727/41/23/234012.

Ostgaard, N., B. E. Carlson, R. S. Nisi, T. Gjesteland, O. Grondahl, A. Skeltved, N. G. Lehtinen, A. Mezentsev, M. Marisaldi, and P. Kochkin (2016), Relativistic electrons from sparks in the laboratory, *J. Geophys. Res. Atmos.*, *121*, 2939–2954, doi:10.1002/2015JD024394.

Rahman, M., V. Cooray, N. A. Ahmad, J. Nyberg, V. A. Rakov, and S. Sharma (2008), X rays from 80-cm long sparks in air, *Geophys. Res. Lett.*, *35*, L06805, doi:10.1029/2007GL032678.

Pasko, V. P., U. S. Inan, and T. F. Bell (1998), Spatial structure of sprites, *Geophys. Res. Lett.*, *25*, 2123–2126.

Raizer, Y. P., and A. N. Simakov (1998), What determines the radius and maximum field at the leader head of long streamers? [in Russian], *Fiz. Plazmy (Plasma Phys. Rep.)*, *24*, 754.

Rakov, V. A., and M. A. Uman (2003), *Lightning Physics and Effects*, Cambridge Univ. Press, New York.

Tarasenko, V. F., and S. I. Yakovlenko (2004), The electron runaway mechanism in dense gases and the production of high-power subnanosecond electron beams, *Phys.-Uspekhi*, *47*, 887–971.

Wang, D., and N. Takagi (2011), A downward positive leader that radiated optical pulses like a negative stepped leader, *J. Geophys. Res.*, *116*, D10205, doi:10.1029/2010JD015391.

Yalandin, M. I., G. A. Mesyats, A. G. Reutova, K. A. Sharypov, V. G. Shpak, and S. A. Shunailov (2011), Limitation of runaway electron beam duration in air-filled gap with inhomogeneous field, *Tech. Phys. Lett.*, *37*, 371–375.

Yalandin, M. I., G. A. Mesyats, A. G. Reutova, K. A. Sharypov, V. G. Shpak, and S. A. Shunailov (2012), Picosecond runaway electron beams in air, *Plasma Phys. Rep.*, *38*, 29–45.